Multidimensional NMR Spectroscopy

DOI: 10.1002/ange.200805612

Single-Scan 2D Hadamard NMR Spectroscopy**

*Assaf Tal, Boaz Shapira, and Lucio Frydman**

Accelerating two-dimensional nuclear magnetic resonance (2D NMR) experiments has been a topic of intense research during the past years.[1] Proposals include exploiting available information by incorporating it into spectrally selective schemes,[2] as well as compressing the 2D NMR experiment into a single-scan by spatially encoding the indirect-domain interactions.[3] Herein we discuss the possibility and consequences of combining these two elements into a single scheme, whereby data are collected while relying on joint spectral/spatial manipulations of the indirect domain. From this emerges a new single-scan 2D Hadamard approach retaining the single-scan nature of "ultrafast" acquisitions, while exploiting known information to achieve a sensitivity improvement. The new two-dimensional radio-frequency (RF) manipulations needed for implementing these experiments, and examples thereof, are described.

2D NMR spectroscopy probes molecular structure and dynamics by correlating shifts along independent axes, based on the traditional time-domain approach [Eq. (1)].[4]

$$\text{Preparation}-\text{Evolution}\ (t_1)-\text{Mixing}-\text{Acquisition}\ (t_2) \qquad (1)$$

A main feature of this method is its scan-by-scan sampling of the t_1 domain, which implies that, regardless of sensitivity considerations, a minimum number of scans needs to be collected for complying with Nyquist criteria along the ν_1 axis. Challenged by this constraint, recent years have witnessed a number of proposals geared at reducing the number of scans needed to retrieve a 2D spectrum. Counted among these proposals is an "ultrafast" approach capable of compressing arbitrary *n*D NMR acquisitions into a single scan.[3] Single-scan 2D NMR spectroscopy replaces the indirect-domain time variable by a spatial encoding of the spin interactions: $t_1(z) = C(z-z_o)$, with C a constant under experimental control. This manipulation, which can be implemented using a variety of RF schemes acting in unison with field gradients,[5] effectively parallelizes the encoding stage of a traditional 2D experiment. Gradient-driven acquisition sequences based on the repetitive unwinding and rewinding of the $\phi_1(z) = C\Omega_1(z-z_o)$ phases evolved by spins at different positions throughout the sample, can then recover the entire 2D data set being sought within a single scan.

An alternative way for accelerating 2D NMR acquisitions arises when the spectral profile expected along the indirect domain is known.[2] In such cases the aim is not necessarily to measure the 2D frequencies (Ω_1,Ω_2) but rather their joint $I(\Omega_1,\Omega_2)$ spectral correlations. Given a number N_{Ω_1} of sites to be correlated along the time-taxing indirect domain it follows that, in principle, no more than N_{Ω_1} independent scans are necessary to obtain this full 2D map.[6] A reduction in the overall acquisition time will then result if the number of sites N_{Ω_1} to be characterized is smaller than the number of N_1 increments needed in a time-domain experiment—a substantial saving when looking for high spectral resolution in sparse data sets. Moreover, it has been demonstrated that if such frequency-based correlations are to be measured, it is convenient to do so using a scheme in which all the sites to be correlated contribute simultaneously according to the dictates of a Hadamard matrix.[2] The ensuing 2D NMR Hadamard approach still requires collecting N_{Ω_1} scans, with each of these containing full contributions of all N_{Ω_1} sites, weighted according to relative phases that switch from 0 to π (Figure 1 A[7]). A final 2D spectra can then be reconstructed by processing the measured signal array using Hadamard and Fourier transforms (HT, FT) along the indirect- and direct-domain frequency axes, respectively.

Figure 1 B presents an alternative approach to implement this kind of acquisition that uses spatial encoding concepts to compress the array involved in the Hadamard weighting into a single NMR scan. This proposal parallelizes the encoding by "partitioning" the sample into N_{Ω_1} individual voxels, and endowing each of these with the spectral profile that would normally arise from an individual scan in a Hadamard-based acquisition. Once the spectral characteristics of the resulting profiles are recovered, standard HT and FT processes could be applied on them to reach the desired 2D results. It would seem, however, that a built-in contradiction is posed by the requirements needed for this kind of manipulation: the Hadamard encoding requires addressing each chemical site according to its Ω_1 spectral shift value, while the spatial encoding of 0/π phases over many distinct portions of the sample requires the application of sizable gradients that will in turn blur any closely spaced chemical shift differences. The problem thus arises of how to achieve, within a "single-shot", both spatial and spectral selectivity with full control over a signal's phase, frequency, and amplitude. A somewhat similar problem arises in the field of medical NMR imaging, when interested in selectively exciting a particular resonance within a confined region in space—for instance when attempting to image the water but not the fat in a certain organ. This procedure is made possible by so-called two-dimensional spatial-spectral pulses;[8] a family of selective RF/gradient manipulations that we propose to exploit for accelerating 2D

[*] A. Tal, Prof. L. Frydman
Department of Chemical Physics, Weizmann Institute of Science
76100 Rehovot (Israel)
Fax: (+972) 8-934-4123
E-mail: lucio.frydman@weizmann.ac.il
Dr. B. Shapira
CCRC, University of Georgia
Athens, GA 30602 (USA)

[**] This research was supported by the Israel Science Foundation (ISF 1206/05) and by the generosity of the Perlman Family Foundation. A.T. acknowledges the Clore Foundation for a Graduate Fellowship.

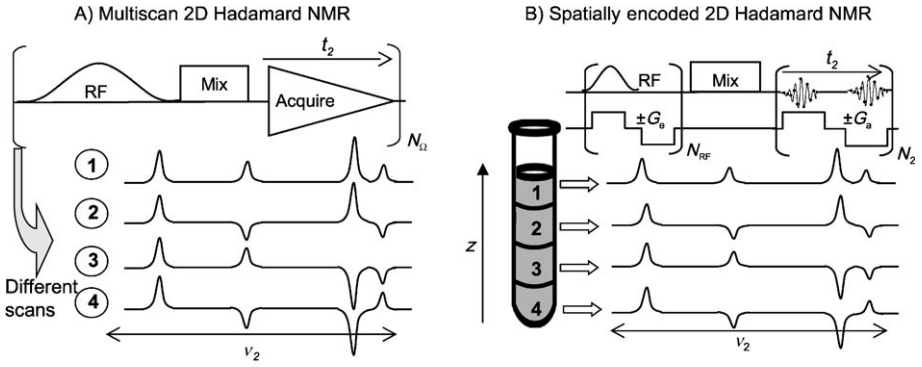

Figure 1. Comparison between: A) The original Hadamard-encoded scheme proposed for obtaining 2D NMR spectra, and B) The single-scan 2D Hadamard approach proposed in this study based on a combined spectral/spatial encoding of the indirect-domain information. Both data are processed on the basis of a Hadamard transfer which weights the spectral set by a matrix—$\begin{pmatrix} 1 & 1 & 1 & 1 \\ 1 & -1 & 1 & -1 \\ 1 & 1 & -1 & -1 \\ 1 & -1 & -1 & 1 \end{pmatrix}$ for the illustrated example—to afford the desired site-resolved information.

NMR spectroscopic acquisitions while relying on both spectral and spatial characteristics. To visualize how a spectral/spatial encoding pulse can be adapted for single-scan 2D Hadamard NMR spectroscopy, it is convenient to analyze its operation in the small-angle excitation regime. The spins' response will then be given by Equation (2).[9]

$$M_{xy}(\omega) \approx i\,\gamma\,M_o\,e^{-i\omega T/2}\int_0^T B_1(t)\,e^{-i\omega t}\,dt \qquad (2)$$

M_o is the longitudinal magnetization prior to the application of the RF, $B_1(t)$ is the pulse's shape, ω is the spins' frequency in a suitable rotating frame, T is the duration of the pulse, and $M_{xy}(\omega)$ is the transverse magnetization at the pulse's end for a particular offset. According to this formalism, spins resonating at a particular ω can be excited by imposing a sinusoidal ω-dependence on the rotating-frame B_1 and, since both $M_{xy}(\omega)$ and $B_1(t)$ are complex quantities, the phase of the $M_{xy}(\omega)$ can be controlled by manipulating the quadrature components of $B_1(t)$. An important aspect of Equation (2) is its independence from the interaction generating the ω distribution, which could equally be due to chemical shifts Ω_1 or due to excitation gradients G_e imparting frequencies according to $\omega = \gamma G_e z$. Spectral/spatial 2D RF pulses exploit this by making the instantaneous ω depend on both shifts and positions, and imposing on ω a time-dependence $\omega(t) = \Omega_1 + \gamma G_e(t) z$ capable of distinguishing the relative contributions of these two terms. The FT in Equation (2) can then be described by a dependence on two independent frequency-defining variables [Eq. (3)],

$$M_{xy}(\Omega_1,z) \approx i\,\gamma\,M_o\,e^{-i[\Omega_1 T + z\,k_1(T)]/2}\int_0^T B_1(t_1)\,e^{i[\Omega_1 t_1 + z\,k_1(t_1)]}\,dt_1 \qquad (3)$$

where $k_1(t_1) = \gamma\int_0^{t_1} G_1(t)\,dt$ is a wavenumber, made time-dependent by the oscillation of the gradient G_e. RF selectivity can thus be tuned to a particular spectral component and to a particular position by designing a time-dependent B_1 pulse, that selectively "resonates" solely with well-defined values of these (Ω_1,z) parameters. Achieving this requires in turn applying an RF pulse while traversing a suitable region in the 2D (k_1,t_1) space: the extent of this (k_1,t_1) excursion will define the resolution achieved along the spectral and spatial axes, while the density of the (k_1,t_1) sampling defines the range of frequency values that can be adequately distinguished. These demands are reminiscent to those involved in spectroscopic imaging acquisitions;[9] indeed the conditions posed by Equation (3) on the (k,t)-space sampling are analogous to those posed by echo-planar spectroscopic imaging (EPSI[10]) for the single-scan sampling of 2D position/shift spectral correlations. Recipes for designing the $B_1(t)$ RF field associated with such (k,t)-space sampling have been discussed in the imaging literature;[8] for the present study the spatial/spectral excitation conditions were implemented using a square-wave $\pm G_e$ gradient oscillating with a period Δt_1 over N_{RF} cycles. The full $T = \Delta t_1 N_{RF}$ duration can thus be used to plan the pulse's excitation of the Ω_1 spectral domain, an excitation which in view of the gradient oscillation eventually becomes a DANTE-like pulse repeating itself along the chemical shift axis at $\left\{\Omega_1 \pm n\,\frac{2\pi}{\Delta t_2}\right\}_{n=0,\pm1,\ldots}$.[11] Thus Δt_1 needs to be made short enough to place unwanted harmonics outside the range of chemical shift interest; at the same time Δt_1 needs to be long enough to support the spatial portion of the selectivity, whose resolution will be defined by $k_{max} = \gamma G_e \Delta t_1/2$. Then, if within each of these $0 \le t' \le \Delta t_1/2$ intervals $B_1(t')$ is shaped with an envelop that matches the desired $M_{spatial}(z)$ spatial profiles, the manipulation proposed in Figure 1B can be achieved. These profiles have to entail a sum of N_{Ω_1} square-like excitations centered at $\left\{z_i = -\frac{L}{2} + \left(i + \frac{1}{1}\right)\frac{L}{N_{\Omega_1}}\right\}_{i=0,\ldots N_{\Omega_1}-1}$ positions, possessing equal $\frac{L}{N_{\Omega_1}}$ thicknesses within a sample of length L and endowed with relative phases of 0 or π as per the dictates of the Hadamard encoding. Moreover, each of the Ω_1 shifts being targeted needs to feel its own Hadamard spatial combination. Fortunately, the linear approximation underlying Equation (3) allows all these complex spatial/spectral multi-voxel/multi-site demands to be fulfilled, by computing the 2D RF pulse required by each spatial and spectral element and then adding up the resulting waveforms. Figure 2 summarizes some of these RF synthesis aspects, and exemplifies its experimental operation for the ^{1}H spectroscopy of a model four-site system placed in a conventional 5 mm NMR probe.

Having imprinted the desired spectral/spatial profile throughout the sample, the Hadamard protocol also requires a way to recover this information from all positions and sites

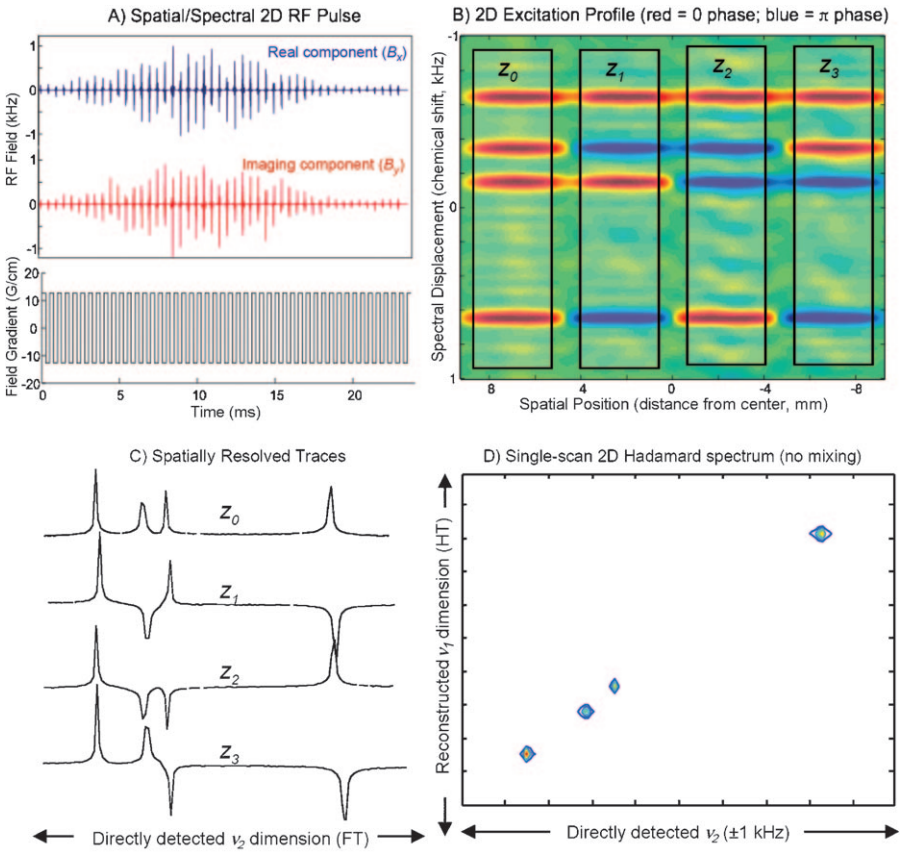

Figure 2. A) 2D spatial/spectral RF excitation pulse needed to generate a Hadamard-encoded profile of the kind depicted in Figure 1 B within a single scan, for the case of four chemical sites coinciding with the ^{1}H resonances of *n*-butylchloride at 500 MHz extending a typical NMR coil length of 19 mm. B) Excitation profile resulting from propagating spins under the gradients and RF in (A), as a function of their positions and chemical shifts. C) Experimental results arising upon adding onto this spatial/spectral encoding profile an EPSI-type decoding, yielding the indicated subspectra over the various $\{z_i\}_{i=0\text{–}3}$ positions throughout the sample. Like all experiments described herein these data were collected on a Varian iNova 500 MHz NMR spectrometer, with all relevant 2D RF waveforms created using custom-written Matlab routines based on the arguments in the text, and imported into the spectrometer for the run. D) Trace arising upon applying a HT to the single-transient profiles indicated in (C), corresponding to a mixing-less 2D NMR correlation.

following an arbitrary mixing process. This is a chemical shift imaging problem, which can be completed within a single transient by relying on an EPSI readout. This stage of the single-scan 2D experiment will be very similar to that underlying the generation of spatial/spectral pulses, except that instead of involving RF-driven manipulations during the excitation, it monitors the direct-domain signals elicited at frequencies Ω_2 from arbitrary positions $-L/2 \le z \le +L/2$. Doing so in a spatially resolved fashion involves collecting the spins' signals while subjecting them to a second round of $\pm G_a$ oscillating gradients with a period Δt_2. This process defines a 2D acquisition space given by $k_2(t_2) = \gamma_a \int_0^{t_2} G_a(t)\,dt$ and t_2; suitable acquisition of the time-domain signal $S(t)$, its rearrangement within the 2D (k_2,t_2) space, and Fourier transforming against these two variables, leads to the z versus Ω_2 map being sought. Splicing the spatial domain data into the $\{z_i\}_{i=0,\ldots N_{\Omega_1}-1}$ slabs that were encoded and subjecting these to the dictates of the HT and FT, leads to the $I(\Omega_1,\Omega_2)$ 2D frequency map being sought. Figure 3 illustrates this with homo- and heteronuclear 2D NMR spectroscopy results obtained on *n*-butylchloride and on a ^{15}N-labeled tripeptide.

Hadamard encoding can shorten the duration of a Nyquist-limited 2D NMR experiment by approximately (N_1 increments)/N_{Ω_1}. Given that ultrafast NMR already compresses 2D acquisitions into a single scan, the question naturally arises of what there is to be gained from an additional Hadamard encoding? The answer is sensitivity. As discussed elsewhere,[12] receiver bandwidths in ultrafast acquisitions need to be widened compared to their conventional counterparts by approximately $N_1 = SW_1 t_1^{max}$, implying a per-scan noise penalty for ultrafast NMR proportional to the square-root of the number of spectral components to be characterized along the indirect domain. On the other hand it is known that for an EPSI acquisition to resolve N_Ω individual spatial voxels as demanded by Figure 2, the receiver bandwidth only needs to increase by this factor versus a conventional spectral acquisition.[9,10] It follows that the sensitivity ratio arising for otherwise identical ultrafast and Hadamard-based single-scan 2D acquisitions will be given by $\sqrt{N_{\Omega_1}/N_1}$. In analogy to what happened in the conventional multi-scan case this sensitivity gain will be modest if the sites to be encoded are many, yet substantial if the indirect domain is sparse and the resolution being sought is high. Figure 4 illustrates this with a comparison between an ultrafast ^{1}H 2D TOCSY NMR spectrum recorded on L-tyrosine under optimal conditions (i.e., optimized spectral widths and filter bandwidths), and a similar Hadamard-based plot obtained following a complex HT. Given the five inequivalent sites observed for this molecule and their spectral separations, theoretical arguments predict a maximum sensitivity gain of approximately 3.0 for the complex HT experiment. In practice an average improvement of 1.8 results from the cross-sectional traces of the different sites (bottom, Figure 4). This deviation is because the number of spatial elements that had to be employed to obtain a "clean" Hadamard characterization exceeded the minimum N_{Ω_1} value by a factor of about 2; in spite of this technical limitation, the potential of the approach is clear. We trust to report on

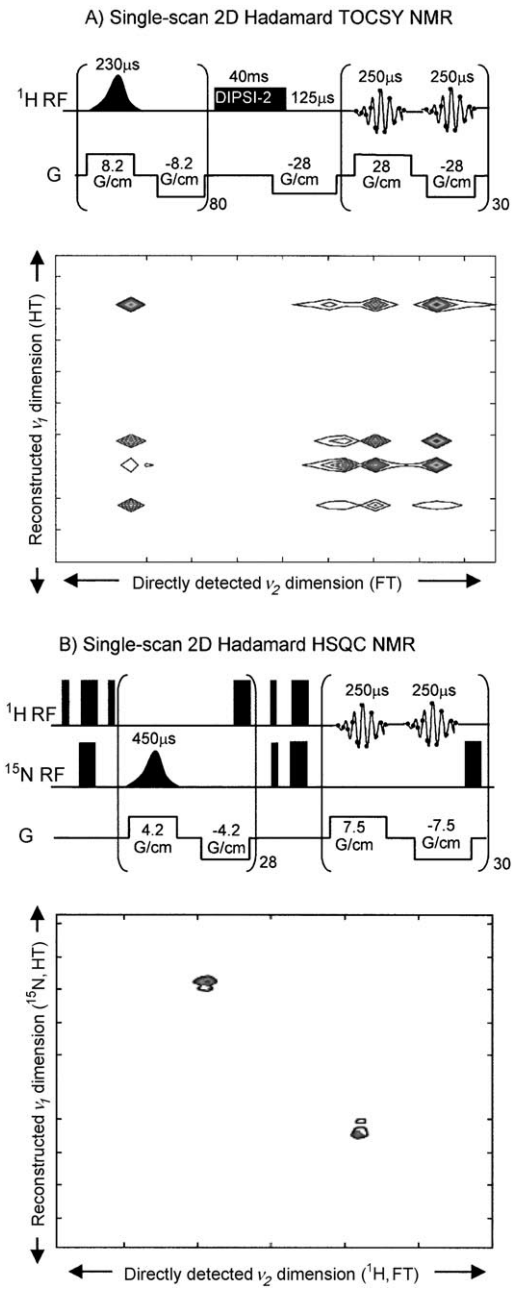

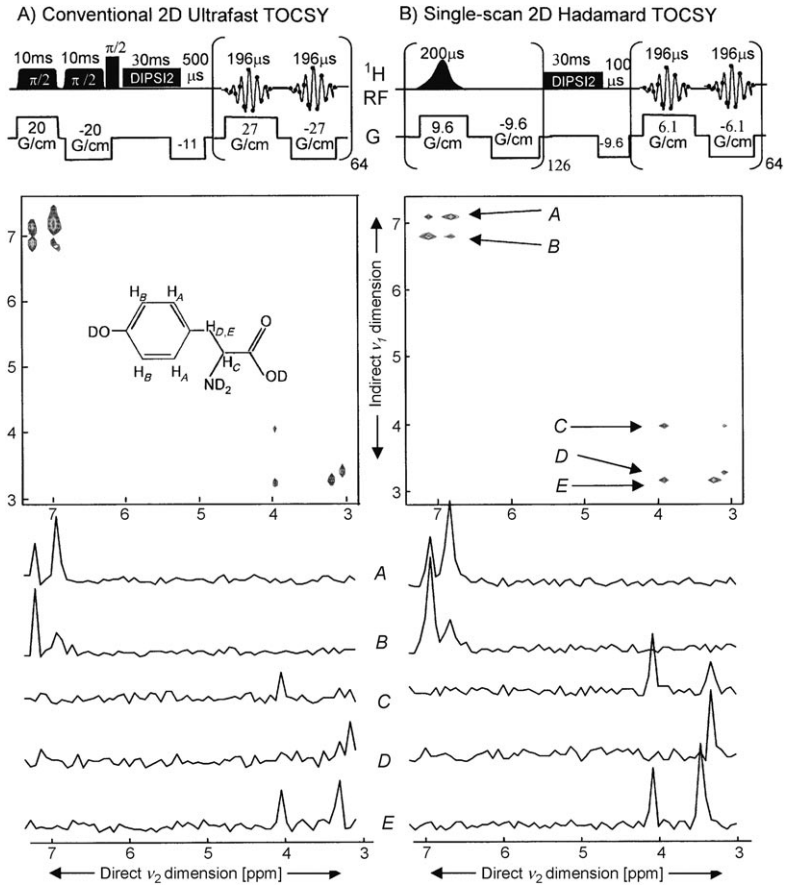

Figure 3. Examples of homo- and heteronuclear single-scan 2D Hadamard experiments on *n*-butychloride (A) and on a model LAF tripeptide (B); in (B) only amide groups were detected. Relevant experimental parameters beyond those indicated included 10 µs dwells for the RF pulse digitization, 2 kHz effective direct-domain acquisition spectral widths, 20 mm effective lengths L, and 5 µs acquisition dwell times. The isotropic mixing bandwidth of the homonuclear experiment was 10 kHz; thick and thin pulses in the heteronuclear experiment denote π and π/2 pulses respectively; π-pulses within the latter's sequence loops were used for the sake of heteronuclear decoupling.

Figure 4. Sensitivity gains brought about by the Hadamard procedure in the ultrafast characterization of sparse spectra, exemplified with 2D TOCSY NMR of a 2 mM L-tyrosine hydrochloride D_2O solution. Top: Pulse sequences used in optimized conventional (left) and Hadamard-based acquisitions (right); further relevant parameters included filter bandwidths of ±108 and ±25 kHz respectively, and 2.4 kHz widths along both domains. Center: Magnitude-mode 2D spectra afforded by each sequence, illustrating the chemical origin of each peak. Bottom: Cross-sections obtained at the indicated arrow positions (plotted at equivalent noise levels) evidencing the sensitivity gains afforded by the Hadamard procedure for different sites.

further possibilities opened up by spectral/spatial RF pulses within purely spectroscopic settings, including ways to overcome the practical losses just referred to by imposing continuous shift-selective spatial patterns chosen to minimize these effects, in upcoming studies.

Received: November 17, 2008
Published online: March 5, 2009

Keywords: Hadamard transform · multidimensional NMR · NMR spectroscopy · spatial/spectral encoding

[1] a) E. Kupče, R. Freeman, *J. Biomol. NMR* **2003**, *25*, 349; b) H. S. Atreya, T. Szyperski, *Methods Enzymol.* **2005**, *394*, 78; c) P. Schanda, B. Brutscher, *J. Am. Chem. Soc.* **2005**, *127*, 8014; d) L. Frydman, *C. R. Chim.* **2006**, *9*, 336.
[2] a) E. Kupče, R. Freeman, *J. Magn. Reson.* **2003**, *162*, 158; b) E. Kupče, R. Freeman, *J. Magn. Reson.* **2003**, *162*, 300; c) E. Kupče, T. Nishida, R. Freeman, *Prog. Nucl. Magn. Reson. Spectrosc.* **2003**, *42*, 95.
[3] a) L. Frydman, T. Scherf, A. Lupulescu, *Proc. Natl. Acad. Sci. USA* **2002**, *99*, 15858; b) L. Frydman, A. Lupulescu, T. Scherf, *J. Am. Chem. Soc.* **2003**, *125*, 9204.

[4] a) J. Jeener, lecture at *Ampere International Summer School II*, Basko Polje, Yugoslavia, September **1971**. Published in N*MR and More in Honor of Anatole Abragam* (Eds.: M. Goldman, M. Porneuf) Les editions de physique, Les Ulis, France, **1994**); b) W. P. Aue, E. Bartholdi, R. R. Ernst, *J. Chem. Phys.* **1976**, *64*, 2229.
[5] Y. Shrot, L. Frydman, *J. Chem. Phys.* **2008**, *128*, 052209.
[6] P. F. Kui, R. Freeman, *J. Magn. Reson.* **1982**, *48*, 519.
[7] "Resolution d'une question relative aux determinants": J. Hadamard, *Bull. Sci. Math.* **1893**, *17*, 240.
[8] a) M. A. Bernstein, K. F. King, X. J. Zhou, *Handbook of MRI Pulse Sequences*, Academic Press, San Diego, **2004**; b) P. A. Bottomley, C. J. Hardy, *J. Appl. Phys.* **1987**, *62*, 4284; c) J. Pauly, D. Nishimura, A. Macovski, *J. Magn. Reson.* **1989**, *81*, 43; d) P. Morris, *Encycl. Magn. Reson.* (Eds.: D. M. Grant, R. K. Harris), Wiley, Chichester, **1996**.
[9] P. Callaghan, *Principles of Magnetic Resonance Microscopy*, Oxford University Press, Oxford, **1991**.
[10] P. Mansfield, *Magn. Reson. Med.* **1984**, *1*, 370.
[11] DANTE (delay alternating with nutation for tailored excitation): see G. Bodenhausen, R. Freeman, G. Morris, *J. Magn. Reson.* **1976**, *23*, 171.
[12] B. Shapira, A. Lupulescu, Y. Shrot, L. Frydman, *J. Magn. Reson.* **2004**, *166*, 152.

